Stability of Nonequilibrium MHD Plasma in the Regime of Fully Ionized Seed

TAKASHI NAKAMURA* AND WOLFGANG RIEDMÜLLER*
Max-Planck-Institut für Plasmaphysik, München, F.R. Germany

The stability of nonequilibrium MHD plasmas in the regime of fully ionized seed, taking into account the ionization of the noble gas, is studied theoretically and experimentally. It is shown that the complete ionization of the seed is attainable with the discharge current and the corresponding electric field able to be achieved in actual MHD generators by reducing the seed fraction down to 10^{-5}. The experimental data show that in the regime of fully ionized seed the plasma is stable in agreement with the theoretical predictions. Effective Hall parameters as high as 6 were obtained, while the effective conductivity remained at the value of the laminar conductivity. The application of this stabilization method to actual MHD generators is discussed.

Introduction

IT is well-known that nonequilibrium plasmas in crossed electric and magnetic fields consisting of alkali seeded noble gas are subject to ionization (or electrothermal) instability.[1,2] Physical interest in the stability of a plasma flow through a magnetic field as well as the possibilities of engineering application of those plasmas in closed cycle MHD electrical power generators motivated a number of proposals for the stabilization of the ionization instability.

One method, proposed by Velichov, Dychne, and Skipuk,[3] is the transmission of an additional current, homogeneously heating the electrons, along the magnetic field. Both theory[4] and experiment[5] show that the current required is too high and stabilization is not very advantageous for practical application.

Another method introducing special conductors to control the potential fluctuations of the most unstable perturbations[3] has not lead, as yet, to definite experimental results.[6]

The addition of a molecular gas has been proposed by Kerrebrock and Draper[7] using excited metastable molecules as an additional homogeneous energy source for the electrons. Unfortunately this stabilizing effect seems to be accompanied by additional energy losses due to inelastic collisions with the molecules.[8] Other means aimed at decreasing the effect of ionization instability are complicated and not yet experimentally verified. Nelson's[9] dynamic stabilization by removing the orientation of the current density vector from the zone of instability during part of an oscillation of an applied HF-field requires rather high additional power densities. Sen's[10] feed-back control provides the stabilization of a single unstable Fourier component only, leaving all other modes unaffected.

Since the observed ionization instability and the anomalous electrical resistivity caused by it are basically linked with the fluctuations of the ionization degree, the method of fully ionizing the seed in order to decouple electron number density and local Ohm's heating seems to be the most simple and promising way to stabilize the plasma.[3]

Nevertheless, there have been few experimental investigations pertaining to noble gases with fully ionized seed in crossed electric and magnetic fields. The first experimental hint for the applicability of this method was given by Belousov, Eliseev, and Shipuk.[11] Later studies, however, presented less optimistic results: Shipuk and Pashkin[12] studied a pulsed discharge with segmented electrodes using argon-cesium and helium-cesium mixtures. They observed that the amplitude of the electron density fluctuations decreased to about 10%, when the electron temperature was increased to a value at which the seed is nearly completely ionized. For argon the discharge structure became irregular. For helium they detected layers almost perpendicular to the current. These layers were assumed to have developed as a result of acoustic instability. In the experiments conducted by Vitshas, Golubev, and Malikov[13] in a disk-shaped electrodeless Hall-type generator, the plasma appeared to be practically homogeneous, particularly in the case of helium with fully ionized cesium. The electron density fluctuations were lower than 3%. Nevertheless, the measured effective Hall parameter values saturated below 2. This saturation can be considered as a sensitive indication of spatial plasma inhomogeneities. The authors assumed a new small scale instability which has not been resolved by their diagnostic methods. Similar results have been reported by Malikov.[14] He used a supersonic linear Faraday generator with an additional pulsed current supplied from an external source to the segmented electrodes. An argon-sodium mixture was studied at conditions near complete ionization of the seed. The critical Hall parameter above which the density fluctuations increased rose up to 4.5, but the measured Hall parameter saturated below 2. The plasma structure was found to be chaotically turbulent.

These disappointing results seemed to confirm the commonly accepted assumption that instabilities in nonequilibrium MHD plasmas are inevitable and no laminar conductivity could be achieved in closed cycle MHD generators.[15]

Apart from the fact that some of the results cited previously are contradictory, all of the experiments have been performed using pulsed discharge plasmas at low gas pressures ($\sim 10^{-1}$ atm) and high seed fractions ($\sim 10^{-3}$). Under those conditions rather high current densities and a strongly elevated electron temperature are required to fully ionize the seed. Furthermore, no experimental data pertaining to effective conductivity in the regime of fully ionized seed have been reported and most of the authors seem to refer to a model of ionization instability neglecting the possibility of the ionization of the noble gas.

Therefore, the purpose of this study is to investigate the stability of nonequilibrium MHD plasmas in a wide range of plasma states covering partially ionized seed, fully ionized seed and partially ionized noble gas. The experimental results pertaining to the bulk electrical properties of the plasma in crossed electric and magnetic fields are given. Seed fractions of the order

Received June 20, 1973; revision received December 3, 1973. This work has been undertaken as part of the joint research program between the Institut für Plasmaphysik and Euratom. The authors are indebted to G. Brederlow for much valuable advice, and to A. Herrle, W. Breitfeld and R. Borde for the construction of the apparatus and assistance in the experiment. The authors also wish to express their gratitude to M. Salvat for his stimulating encouragement.

Index categories: Plasma Dynamics and MHD; Electric Power Generation Research; Atomic, Molecular, and Plasma Properties.

* Scientist.

of 10^{-5} have been chosen so as to achieve complete ionization at current densities and electric field strengths which approximate those expected in actual MHD generators.

Theory

The stability of nonequilibrium plasmas with arbitrary degree of ionization of the seed has been studied by several authors[2,16-18] by means of linear perturbation analysis. The following is an extension of the linear theory by allowing for partial ionization of the noble gas. Considered is the usual set of equations defining the state of a plasma with elevated electron temperature. The study is limited to frequencies and wavelengths such that the low magnetic Reynolds number approximation is valid and quasineutrality can be assumed. Therefore

$$\text{rot}\,\mathbf{E} = 0, \qquad \mathbf{B} = \text{const}$$
$$\text{div}\,\mathbf{j} = 0, \qquad n_e = n_i$$

where $\mathbf{E}$, $\mathbf{j}$, $\mathbf{B}$ are the electric field, current density and magnetic induction vectors, and n_e, n_i are the electron and ion number densities. The state of the heavy gas is supposed to be steady and uniform. Hence only the electron gas equations should be considered.

Because the electrons mainly contribute to the transport of electricity, ion slip can be neglected and Ohm's law can be written

$$\mathbf{j}+\mathbf{j}\times\boldsymbol{\beta} = \sigma\left(\mathbf{E}+\mathbf{v}_g\times\mathbf{B}+\frac{1}{n_e e}\text{grad}\,p_e\right)$$

where $\boldsymbol{\beta} = \beta(\mathbf{B}/B)$, β being the electron Hall parameter, σ is the scalar electrical conductivity and $p_e = n_e kT_e$ is the electron pressure.

Finally, the time variation of the (thermal and potential) energy of the electron gas $\varepsilon_e = n_e \frac{3}{2}kT_e + n_{N^+}\varepsilon_N + n_{S^+}\varepsilon_S$

$$\frac{\partial}{\partial t}\varepsilon_e + \text{div}\,(\mathbf{v}_e\varepsilon_e) + p_e\,\text{div}\,\mathbf{v}_e = \frac{j^2}{\sigma} - A - Q_r - \text{div}\,\mathbf{q}_e$$

Here ε_N, ε_S and n_{N^+}, n_{S^+} are the ionization energies and the ion number densities of the seed and the noble gas component, $\mathbf{v}_e$ is the electron drift velocity, A is the energy loss due to elastic collisions

$$A = \sum_i n_e 2(m_e/m_i)\nu_{ei}\tfrac{3}{2}k(T_e - T_g)$$

where ν_{ei} is the collision frequency for energy exchange between electrons and the ith heavy species with the mass m_i. Energy losses associated with radiation Q_r and heat conduction $\text{div}\,\mathbf{q}_e$ are included.

The rates of ionization and recombination by electron impact are assumed to be fast enough so that a Saha equilibrium for the electron density is valid:

$$n_{S^+}\cdot n_e/[(n_S)_o - n_{S^+}] = \frac{2g_{S^+}}{g_S}\left(\frac{2\pi m_e kT_e}{h^2}\right)^{3/2}\exp\left(-\frac{\varepsilon_S}{kT_e}\right)$$
$$n_{N^+}\cdot n_e/[(n_N)_o - n_{N^+}] = \frac{2g_{N^+}}{g_N}\left(\frac{2\pi m_e kT_e}{h^2}\right)^{3/2}\exp\left(-\frac{\varepsilon_N}{kT_e}\right)$$
$$n_e = n_{S^+} + n_{N^+}$$

$(n_S)_o$ and $(n_N)_o$ are the total number densities and the g's are the statistical weights of the seed and noble gas atoms and ions.

Note that two Saha equations are sufficient only if argon, with its relatively low ionization energy, $\varepsilon_A = 15.75$ ev, is the noble gas. In the case of helium-cesium mixtures, the second ionization of cesium must be taken into account due to the small difference between the ionization energies, $\varepsilon_{He} = 24.58$ ev and $\varepsilon_{Cs} = 25.1$ ev.

The essential difference between this and earlier calculations[16-18] is a more complete description of the relationship between electron density and electron temperature in this model. Therefore, we can transfer immediately the known result for the growth rate of a Fourier component of a disturbance in an initially homogeneous plasma. In the limit of wavelengths which are large in comparison with the characteristic length associated with dissipation due to heat conduction and radiation and taken at an angle of the wave vector which gives the maximum growth rate, the result[18] is

$$\omega_i = \frac{1}{\tau^*}\{[(\beta n_T)^2+\sigma_T{}^2]^{1/2} - [(\beta_{cr}n_T)^2+\sigma_T{}^2]^{1/2}\}$$

where

$$n_T = (d\ln n_e/d\ln T_e) \quad \text{and} \quad \sigma_T = (d\ln\sigma/d\ln T_e)$$

are the logarithmic derivatives of the electron density and the electrical conductivity with respect to the electron temperature at steady-state conditions. The characteristic time is

$$\tau^* = \frac{\tfrac{3}{2}kT_e n_e(1+n_T)+\varepsilon_S(n_S)_o\alpha_S(1-\alpha_S)[\tfrac{3}{2}+(\varepsilon_S/kT_e)-n_T]+\varepsilon_N(n_N)_o\alpha_N(1-\alpha_N)[\tfrac{3}{2}+(\varepsilon_N/kT_e)-n_T]}{j^2/\sigma}$$

where α_S and α_N are the degrees of ionization of the seed and the noble gas, respectively. The familiar result[1] for the critical Hall parameter above which the instability appears is

$$\beta_{cr} = [(A_T{}^2-\sigma_T{}^2)/n_T{}^2]^{1/2}$$

where $A_T = d\ln A/d\ln T_e$ is the logarithmic derivative of the electron energy loss term. The dependence of the electron density on the electron temperature[19] becomes

$$n_T = \frac{\alpha_S(n_S)_o(1-\alpha_S)[\tfrac{3}{2}+(\varepsilon_S/kT_e)]+\alpha_N(n_N)_o(1-\alpha_N)[\tfrac{3}{2}+(\varepsilon_N/kT_e)]}{\alpha_S(n_S)_o(2-\alpha_S)+\alpha_N(n_N)_o(2-\alpha_N)}$$

Based on this model we have calculated the critical Hall parameter for various gas mixtures and gas parameters. A typical result is shown in Fig. 1. Here β_{cr} is plotted as a function of the electron temperature for argon-potassium mixtures. In case of the highest seed fraction, the plasma with fully ionized seed is unstable even without a magnetic field (thermal instability, called static by Solbes[18]) due to the relative importance of the Coulomb collisions. As the seed fraction decreases, the maximum critical Hall parameter increases, partially because of the reduced influence of the Coulomb collisions but mostly due to the reduced value of n_T, in other words, because the electron density plateau in the regime of fully ionized seed becomes flatter if the partial pressure of the seed is reduced. Hence the reduction of the seed fraction, thus the reduction of electron temperature necessary for complete ionization, improves the stability of the plasma.

Figure 2 shows the critical Hall parameter as a function of the current density for argon-cesium mixtures. Here the maximum values are higher than in the foregoing example, due to the larger difference between the ionization energies of the seed and the noble gas. Note that there exist only narrow limited current density regimes where a high critical Hall parameter is available.

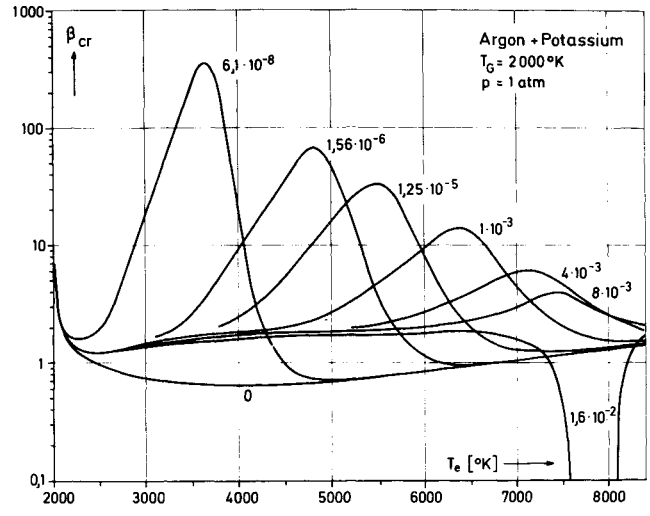

Fig. 1 Critical Hall parameter vs electron temperature for various seed fractions calculated for argon-potassium plasma.

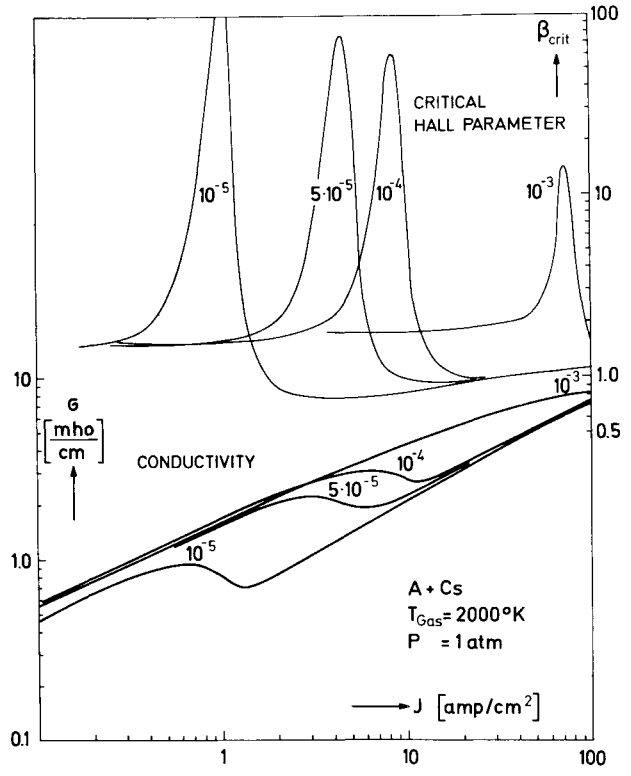

Fig. 2 Critical Hall parameter and electrical conductivity vs current density for various seed fractions calculated for argon-cesium plasma.

An exact control of the discharge parameters, therefore, will be necessary in order to establish experimentally nonequilibrium plasmas with fully ionized seed in a regime where stability is expected.

Experimental Apparatus

It is evident from the foregoing theoretical study that the requirements vital to the experimental study are the obtaining of a homogeneous, constant seed fraction of the order of 10^{-5} and the accurate controlling of the discharge current so as to reach the desired plasma state.

Cesium was chosen as the seed material partly because of its high vapor pressure at temperatures at which the seed supply system can operate without excessive complications. In order to ensure homogeneous current discharges, simulated Faraday geometry was chosen as the test section configuration because in this configuration the Lorentz force is more properly compensated for by the pressure gradient than in the longitudinal discharge configuration. Provisions were made to lower the gas pressure in the test section in order to achieve meaningfully high Hall parameters with the magnetic fields available.

The noble gas is heated by an arc heater and flows into the mixing duct where the cesium vapor is injected. The two components are mixed as the gas flows through the mixing duct. For the experiments using the helium-cesium mixture, mixing grids made of aluminum oxide were installed. This was necessary in order to obtain homogeneous mixing because the flow in the duct was laminar. After the gas leaves the test section, it goes through a cooler, a seed removal filter and then is evacuated from the system by an exhaust pump.

The test sections used for experiments on argon-cesium and helium-cesium mixtures are shown in Fig. 3. The test section for argon-cesium mixture has a cross section of 2×1.7 cm^2 and effective length of 8.6 cm. Two thermocouples are installed upstream and downstream of the discharge section. Fifteen pairs of electrodes, each of which is made of 1-mm-diam tungsten wire, are located at the upper and lower walls of the channel. The first four electrodes have a height to pitch ratio of 5 and the other 11 electrodes have height to pitch ratio of 10. This large height to pitch ratio was chosen in order to minimize the uncertainty of the current direction in the region where probes are located. A pair of preionizers is placed in the gas flow at 1 cm upstream from the first electrode pair. Three pairs of electrodes, made of 2 mm tungsten wire, are placed in the gas flow at the inlet and outlet of the test section for longitudinal discharge. Six potential probes are inserted into the channel from a side wall. Each probe is made of 0.8-mm-diam tungsten wire and has an effective length of 5.5 mm. Three small scale probes, made of tungsten wires, 0.3 mm in diam and 2 mm in length, are inserted into the channel from the opposite side wall. These small scale probes, placed 2 mm apart in two directions, are installed to detect local electric field fluctuations. An optical window, 5-mm-diam holes on both side walls, is located between probes for spectroscopic measurements of the plasma.

The test section configuration used for helium-cesium mixture is the result of considerable experience gained with other configurations. In the initial stage of experiments using helium-cesium mixture, severe heating of electrodes was encountered. The tungsten anodes were melted by the discharge current while the tungsten cathodes remained intact. This severe heating of the anodes was caused by high joule heating in the vicinity of the electrode surface where the discharge current concentrates. In addition to heat transfer from locally heated gas, anodes also receive kinetic energy of the incoming electron plus the effective work function of the anode surface. As for the cathodes, emitted electron flux carries off the effective work function of the cathode surface, thereby compensating for the heat input. This anode heating is particularly significant in the case of the helium-cesium mixture because of high joule heating and high thermal conductivity.

To circumvent the electrode heating problem, the present test section equipped with heat sink type electrodes was developed. The dimension of this test section is the same as before but the configuration of the test section is simplified. Here only 12 pairs of electrodes, six potential probes and two thermocouples are installed. Cathodes are made of 2-mm-diam tungsten rods and anodes are made of tungsten blocks each having a volume of 0.22 cm^3. With this heat capacity anode temperature elevation during the discharge time of 2 sec was limited to about 100°K.

To determine the electron temperature and density, measurements of the cesium recombination continuum[20] were conducted. Special care was taken to separate the cesium recombination continuum from the line radiations of argon, helium, cesium and possible impurities. Consequently, two narrow band interference

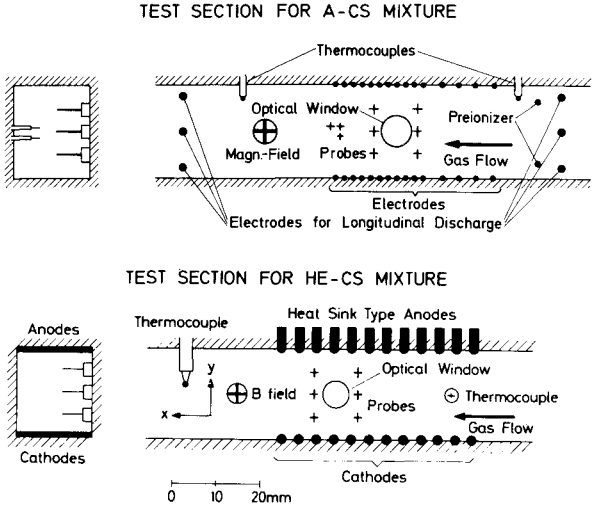

Fig. 3 Test sections used for experiments on argon-cesium and helium-cesium mixtures.

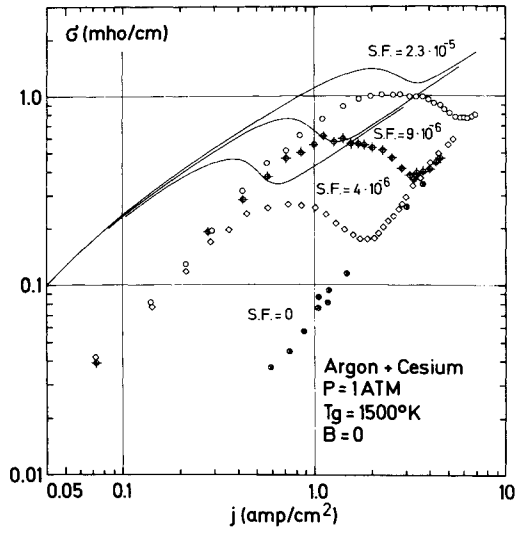

Fig. 4 Comparison of theoretical and experimental electrical conductivity of argon-cesium plasma vs current density for various seed fractions.

filters having transmission wavelengths of 4228 Å and 4857 Å with band width of 10 Å were chosen.

The experiments using argon-cesium mixture were conducted at 1 atm pressure and at gas temperature of 1500°K. The seed fraction was varied over a range from 0 to 2.3×10^{-5}. The gas velocity in the test section was in a range from 60 m/sec to 100 m/sec which corresponds to the plasma residence time of 400 μsec to 650 μsec. The experiments using helium-cesium mixture were conducted at low pressure, 0.2 atm, in order to achieve meaningfully high Hall parameter with the available magnetic field ($B \lesssim 2.3$ Tesla). The seed fraction was controlled over a range from 1.2×10^{-5} to 2×10^{-4}. The gas temperature at the inlet of the test section was 1000°K and the gas velocity was 130 m/sec which corresponds to the plasma residence time of 350 μsec.

Each electrode pair was connected independently to d.c. power supply through a current regulator equipped with power transistors. This electronic current regulator made it possible to control the discharge current independent of the plasma impedance. For the experiments using helium-cesium mixture, the discharge current through each electrode pair was regulated linearly in time from the minimum current (~ 0.3 amp) to the maximum current (~ 5 amp) and then back to the minimum current in 2 sec while the magnetic field was held constant. This was to limit the elevation of anode temperature. The joule heating of the gas was noticeable. With the maximum discharge current, 5 amp for each electrode pair, the gas temperature increased from the inlet to the outlet of the test section by about 400°K. In the case of argon-cesium plasma there was no restriction on the discharge time, therefore it was possible to hold the discharge current constant and vary the magnetic field. There was no significant elevation in gas temperature in this case.

Experimental Results

The experimental investigations were conducted first on argon-cesium mixture because it was relatively easy to work with as described in the previous section. The elaborate test section configuration for this mixture enabled us to obtain more detailed and precise results regarding the stability of nonequilibrium MHD plasma. The experimental investigation on helium-cesium plasma was subsequently conducted to provide complementary experimental results.

As the first step of the experiments, measurement of electrical conductivity without the applied magnetic field was performed. The electrical conductivity was determined from the measured electric field between probes for a given current density which is the total discharge current divided by the discharge cross section of the channel. The values of the electrical conductivity of argon-cesium and helium-cesium plasma are plotted against the current density for several seed fractions in Fig. 4 and Fig. 5.

For a given seed fraction the conductivity increases as the current density increases until full ionization of the seed is achieved. Thereafter the conductivity decreases as the electron temperature increases while the electron density remains constant. The conductivity increases again when ionization of the noble gas is initiated. This conductivity reversal is clearly visible in argon-cesium plasma (Fig. 4) whereas it is not as pronounced in helium-cesium plasma (Fig. 5). This is due to the elevation of helium gas temperature caused by high joule heating which compensates for the reduction of the conductivity in the regime of fully ionized seed. In each figure theoretical conductivity values are shown in solid lines.

The electrical conductivity and Hall parameter were calculated according to the modified Frost's mixture rule.[21-24] The speed dependent electron-atom cross sections of argon and helium given by Frost and Phelps[25] are used. The electron-cesium cross section was taken as constant, 2.5×10^{-14} cm^2, because of the small seed fraction. The radiation energy loss from the resonance lines of cesium are included.

In the case of argon-cesium plasma considerable discrepancy exists between theoretical and experimental values. This discrepancy is partly due to the radiation losses that are not included in the calculation, namely the radiation losses other than the resonance radiation of the neutral seed atoms. It is obvious from Fig. 4 that the radiation energy loss from excited argon atoms is important in the electron energy balance.

The discrepancy is also due to the uncertainty of the value of electron-argon cross section. As will be shown in Fig. 6, measurements of Hall parameter show that the present electron-argon cross section gives a value about 30% higher than the experimental value. This is about the same amount of discrepancy between theoretical and experimental conductivity in the regime of fully ionized seed.

In the case of helium-cesium plasma (Fig. 5) the agreement between theoretical and experimental values is good. This is because the relative importance of electron energy loss through radiation is small and because the electron-helium collision cross section is of a well-behaving nature. The small discrepancy between the theoretical and the experimental values can readily be explained by the elevation of the gas temperature due to high joule heating.

In order to determine the seed fraction and to identify the plasma state, measurement of the Hall parameter in a weak diagnostic magnetic field together with the measurement of recombination continuum radiation were conducted for each different experimental condition. In Fig. 6 the results obtained

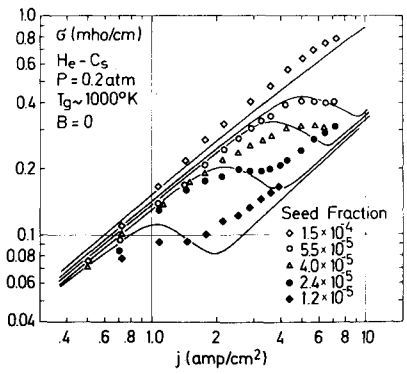

Fig. 5 Comparison of theoretical and experimental electrical conductivity of helium-cesium plasma vs current density for various seed fractions.

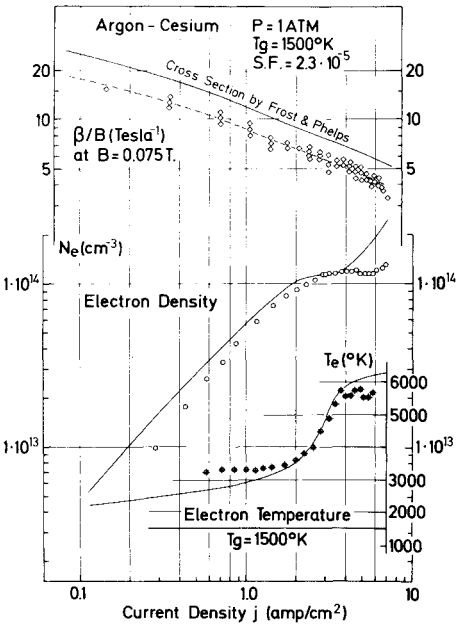

Fig. 6 Comparison of theoretical and experimental Hall parameter, electron density and electron temperature of argon-cesium plasma vs current density in a weak, diagnostic magnetic field.

with argon-cesium plasma are shown. On the upper part of Fig. 6 the electron mobility β/B is plotted. The diagnostic magnetic field was limited to the value such that $\beta < \beta_{cr}$. In reducing β in the plasma from the apparent value, it is necessary to know the angle of the turning of the current vector in a magnetic field due to the finite segmentation. The effective Hall parameter β_{eff} and the effective conductivity σ_{eff} are related to the apparent values, $\beta_{\text{app}} = E_x/E_y^*$ and $\sigma_{\text{app}} = j/E_y^*$ where $E_y^* = (\mathbf{E} + \mathbf{v}_g \times \mathbf{B})y$, through the relations derived from Ohm's law

$$\beta_{\text{eff}} = (\beta_{\text{app}} - \tan\varphi)/(1 + \beta_{\text{app}} \tan\varphi), \quad \sigma_{\text{eff}} = \sigma_{\text{app}}(1 - \beta_{\text{eff}} \tan\varphi)$$

where $\tan\varphi = j_x/j_y$. Due to the boundary condition at the

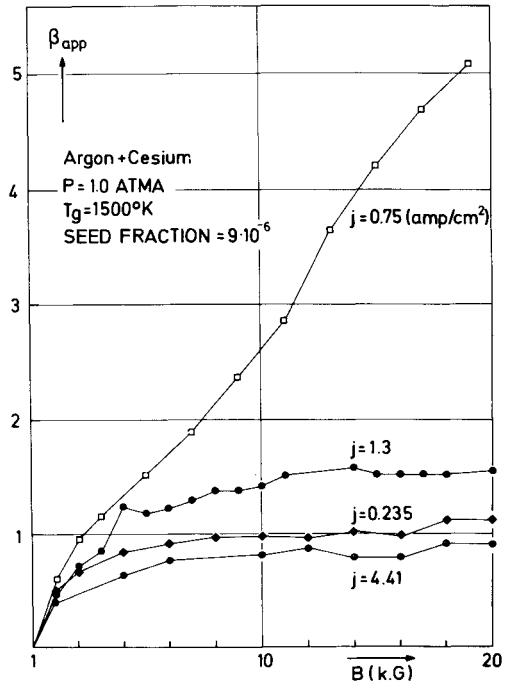

Fig. 7 Apparent Hall parameter of argon-cesium plasma vs magnetic field for several current densities.

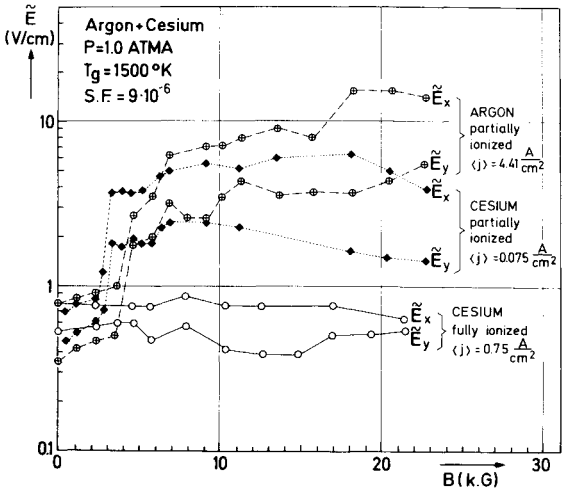

Fig. 8 Amplitude of the electric field fluctuation in argon-cesium plasma vs magnetic field.

electrode surfaces the current turns such that $\tan\varphi < 0$ which means $\beta_{\text{eff}} > \beta_{\text{app}}$ and $\sigma_{\text{eff}} > \sigma_{\text{app}}$. The turning of the current vector in a magnetic field, $\tan\varphi$, should be assessed from the test section configuration. In a weak diagnostic magnetic field as in the case of Fig. 6, however, σ_{eff} may be substituted by σ_o. Then β_{eff} can be solved without specifying $\tan\varphi$. The values of β shown in Fig. 6 are those of β_{eff} determined in this manner.

The electron density shown in Fig. 6 was determined from the experimentally obtained values of β/B. The experimentally obtained electron density values remain constant between $j \approx 3$ amp/cm^2 and 6 amp/cm^2. The electron temperature determined from the ratio of intensities of the recombination continuum at two different wavelengths rises sharply as the electron density is saturated. It is obvious from these data that full ionization of the seed is achieved with current density between 3 amp/cm^2 to 6 amp/cm^2.

The seed concentration was determined to be the electron density value at the plateau, $n_e = 1.2 \times 10^{14}$ cm^3, which corresponds to the seed fraction of 2.3×10^{-5}.

The intensity of the recombination continuum was calibrated to the electron density determined by this method so that it was possible to determine the electron density optically in a strong magnetic field.

Theoretical values of β/B, n_e and T_e for the corresponding plasma are shown by solid lines. As mentioned before, theoretical values for β using the electron-argon cross section by Frost and Phelps are from 30% to 40% higher than the experimental values. For n_e and T_e good agreement exists between theoretical and experimental values. This is because of the fact that the magnitude of the electron-argon cross section does not have a direct influence on the calculation of n_e and T_e as function of j. The shift of the electron density plateau towards higher current density is the effect of radiation loss from excited argon atoms.

In Fig. 7, β_{app} for several current densities, hence for several degrees of ionization obtained in argon-cesium plasma, are plotted against B. The values of β_{app} for the lowest current density, $j = 0.24$ amp/cm^2, represent the plasma state in which the seed is partially ionized. At this condition β_{app} is saturated at around 1.0. The amplitude of the electric field fluctuation measured in the same plasma state, $j = 0.075$ amp/cm^2 (shown in Fig. 8), increases suddenly at $B \approx 0.3$ Tesla. This indicates the onset of ionization instability as expected in this plasma state.

For higher current density, $j = 0.75$ amp/cm^2, β_{app} does not saturate but keeps increasing up to a value of 5 at $B = 1.8$ Tesla. The amplitude of the electric field fluctuation in this plasma state remains constant as shown in Fig. 8. By measuring the recombination continuum in the magnetic field this plasma state

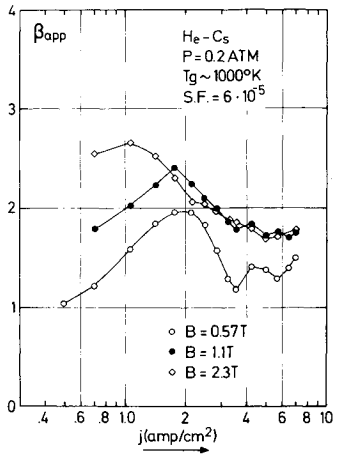

Fig. 9 Apparent Hall parameter of helium-cesium plasma vs current density for three different magnetic fields.

was identified to be the regime of fully ionized seed. It should be noted that at $j = 0.75$ amp/cm^2 the degree of ionization for $B = 0$ is less than unity as can be seen from Fig. 4. However, the degree of ionization increases to unity (at the same current density) as B increases because the laminar conductivity σ_B decreases due to the strong variation of the electron argon cross section.

As the current density is increased further the plasma becomes unstable due to the ionization of noble gas. At $j = 1.3$ amp/cm^2, β_{app} saturates at less than 1.0. The amplitude of the electric field fluctuation increases suddenly at around $B = 0.4$ Tesla. The typical frequency of the electric field fluctuation is about 10 kHz.

To visualize the transition of the plasma states it is useful to plot β_{app} against j for a constant magnetic field. In Fig. 9, β_{app} measured in helium-cesium plasma is plotted against j for three different magnetic fields. For $B = 0.57$ Tesla, $\beta_{app} = 1.0$ at $j = 0.5$ amp/cm^2 while theoretical β for this plasma state is about 2.5. As j is increased, i.e., as degree of ionization is increased, β_{app} increases up to 2 at $j \approx 2$ amp/cm^2, thereafter it decreases as the ionization of helium is initiated. This characteristic is also true for higher magnetic fields ($B = 1.1T$ and $2.3T$). From the recombination continuum measurements the state of the plasma at which β_{app} takes maximum value was identified as the state of fully ionized seed for each magnetic field strength.

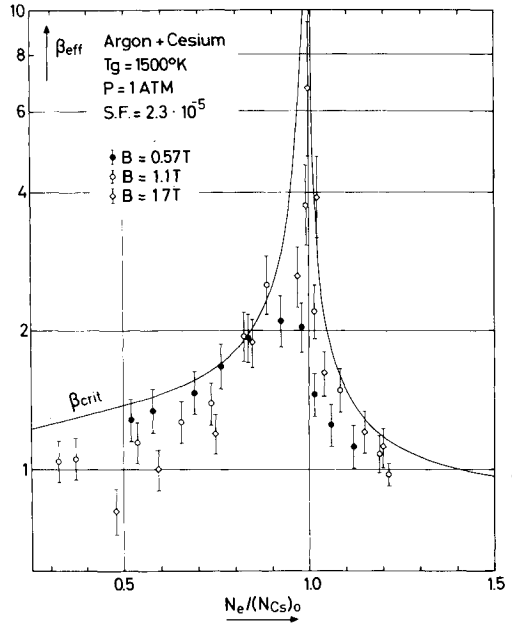

Fig. 10 Effective Hall parameter of argon-cesium plasma vs degree of ionization for various magnetic fields.

It should be noted, however, that for the same seed fraction full ionization of the seed without the magnetic field is achieved at a higher current density of about 5 amp/cm^2 as can be seen from Fig. 5. This relatively large discrepancy for helium-cesium plasma cannot be ascribed to the reduction of σ_B which is not more than 7%. It cannot be ascribed to the reduction of the seed concentration due to the pressure change upstream of the test section caused by $\mathbf{j} \times \mathbf{B}$ force. The maximum change in seed fraction, which was considerable for shorter discharge time, for the present condition is estimated to be less than 10%. A possible reason for this effect is that when the magnetic field is applied, the discharge current flows between electrodes in constricted paths without filling the total volume of the test section. In this case the actual current density is higher than the calculated value.

In order to identify the stability of the plasma in terms of a more meaningful plasma parameter, an attempt was made to plot the effective Hall parameter against the degree of ionization.

In Fig. 10, β_{eff} measured in argon-cesium plasma is plotted against $\langle n_e \rangle / (n_{cs})_o$ where $\langle n_e \rangle$ is the spatially averaged electron density determined from the intensity of the recombination continuum and $(n_{cs})_o$ is the total (ionized and neutral) seed density. As mentioned before β_{eff} is always larger than β_{app}. In order to calculate β_{eff} from β_{app} the direction of the discharge current has to be known. Here the maximum turning of the discharge current is assumed to be the pitch to height ratio of the test section. In Fig. 10 upper limit to β_{eff} is calculated from β_{app} assuming $\tan \varphi = -s/h = -0.1$. The lower limit to β_{eff} gives the value of β_{app} actually measured. This also applies to the conductivity data shown in Fig. 12. The theoretical value of β_{cr} based only on the collisional damping, i.e., the value of β_{cr} for an infinite wavelength, is shown by a solid line. The envelope of data points for β_{eff} represents the experimental value of β_{cr}. The agreement between theory and experiment is excellent despite the fact that the effect of the boundary and the finite wavelength are not included in the calculation of β_{cr}.

The behavior of the effective conductivity σ_{eff} is yet to be clarified. It is meaningful to compare σ_{eff} to the laminar conductivity σ_B at the same plasma condition. In calculating σ_B, its reduction due to the magnetic field should be taken into account.

In Fig. 11 the theoretical value of σ_B/σ_o is plotted against β both for argon-cesium and helium-cesium plasma, where σ_B is the laminar conductivity with the magnetic field and σ_o is that without the magnetic field. For helium-cesium plasma the reduction is small ($\sim 7\%$) because the speed dependent electron-helium cross section is constant in wide range. For argon-cesium plasma, however, the reduction is significant ($\sim 30\%$) because of the strong Ramsauer effect. This reduction is particularly pronounced for the present low seed fraction (S.F. $\approx 10^{-5}$) because electron-argon collision is dominant among electron-heavy species collisions whereas for the normal seed fraction (S.F. $\approx 10^{-3}$) electron-argon collision plays a minor role.

In Fig. 12 $\sigma_{eff}/\sigma_B(\langle n_e \rangle)$ for argon-cesium plasma is plotted against $\langle n_e \rangle / (n_{cs})_o$ for three different B where $\sigma_B(\langle n_e \rangle)$ is the

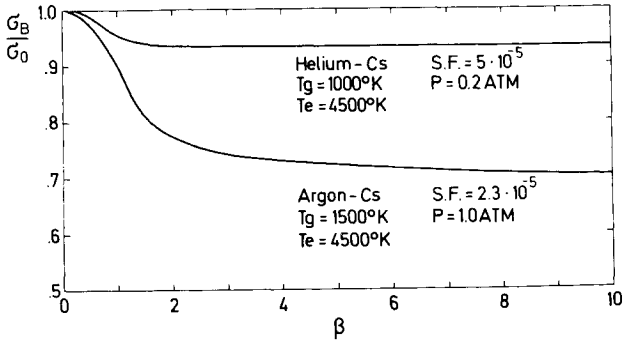

Fig. 11 Reduction of laminar conductivity transverse to the magnetic field vs Hall parameter for helium-cesium and argon-cesium plasma.

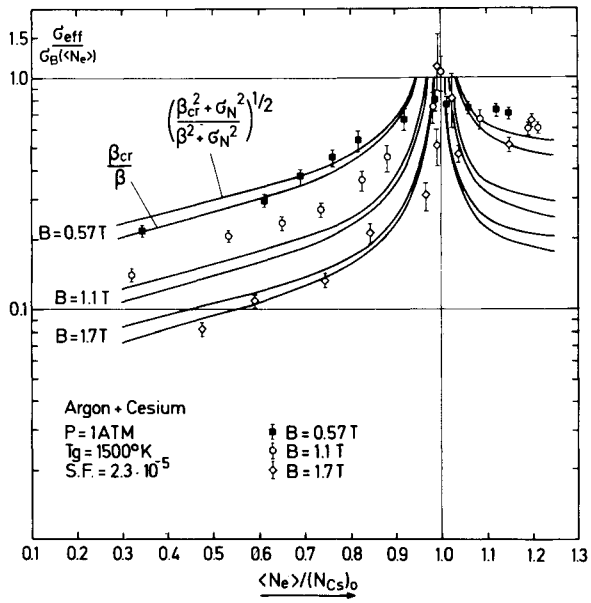

Fig. 12 Effective conductivity of argon-cesium plasma vs degree of ionization for three different magnetic fields.

laminar conductivity of the magnetized plasma evaluated at $\langle n_e \rangle$. In order to avoid the uncertainty of the magnitude of electron-argon cross section, $\sigma_B(\langle n_e \rangle)$ was determined from the experimental conductivity without the magnetic field, $\sigma_o(\langle n_e \rangle)_{\text{exp}}$, multiplied by the theoretical reduction factor σ_B/σ_o.

The effect of stabilization is conclusively demonstrated in Fig. 12. As $\langle n_e \rangle/(n_{cs})_o$ increases to unity, $\sigma_{\text{eff}}/\sigma_B(\langle n_e \rangle)$ also approaches unity. At $\langle n_e \rangle/(n_{cs})_o = 1$, $\sigma_{\text{eff}}/\sigma_B(\langle n_e \rangle)$ reaches unity indicating total suppression of ionization instability in the regime of fully ionized seed. At this plasma state the measured electron and gas temperatures give $T_e/T_g \approx 3$. In order to investigate the possibility that ion acoustic wave might be amplified[26] when $T_e/T_g > 3.5$, the gas temperature was lowered to 1000°K so that $T_e/T_g \approx 4.5$ in the regime of fully ionized seed. The results obtained for lower gas temperature were the same as for higher gas temperature.

In Fig. 12 the theoretical expression for σ_{eff} as given by Solbes[27]

$$\frac{\sigma_{\text{eff}}}{\langle \sigma \rangle} = \left(\frac{\beta_{cr}^2 + \sigma_N^2}{\langle \beta \rangle^2 + \sigma_N^2} \right)^{1/2} \qquad \sigma_N = \frac{d \ln \sigma}{d \ln n_e}$$

and the empirical formula of the form[5,28]

$$\frac{\sigma_{\text{eff}}}{\langle \sigma \rangle} = \frac{\beta_{cr}}{\langle \beta \rangle}$$

are also given in solid lines, making approximations $\langle \sigma \rangle = \sigma_B(\langle n_e \rangle)$ and $\langle \beta \rangle = \beta(\langle n_e \rangle) = \beta$. These two expressions give nearly the same value and the agreement between them and the experimental value is satisfactory.

Conclusions

From the experimental evidences given in the foregoing section it is concluded that ionization instability in nonequilibrium MHD plasmas can be suppressed by fully ionizing the seed in accordance with the theoretical prediction given in this paper.

For argon-cesium and helium-cesium mixtures in a simulated Faraday geometry, full ionization of the seed was obtained at moderate electron temperature elevation and an electric field strength readily achieved in MHD generators by reducing the seed fraction down to the order of 10^{-5}. In the regime of fully ionized seed effective Hall parameter of the order of 6 and effective conductivity equal to the laminar conductivity were obtained, while the amplitude of the electric field fluctuations did not increase with the applied magnetic field. Up to an electron temperature elevation of $T_e/T_g = 4.5$ no deterioration of the bulk electrical properties of the plasma was observed in the regime of fully ionized seed. It was shown that the ionization of the noble gas limits the range of stable plasma state.

The application of this stabilization method provides possibilities to increase the local power density and efficiency of nonequilibrium MHD generators operating with high Hall parameter. A preliminary calculation[19] indicates that the local power density of the Faraday generator can be increased up to an order of magnitude. The Hall generator operating with stable plasma could yield high local efficiency.

In applying this stabilization method to actual MHD generators the characteristic of load circuit must be carefully matched to the current-voltage characteristic of the magnetized plasma in order to attain the regime of fully ionized seed. Electrode phenomena, namely higher effective work function of electrodes and high joule heating in the vicinity of electrode surface, may pose serious problems. On the other hand, the reduction of the seed concentration down to the level of impurity of the working gas ($\sim$10 ppm) promises technological as well as economical advantages.

References

[1] Velichov, E. P. and Dykhne, A. M., "Plasma Turbulence due to the Ionization Instability in a Strong Magnetic Field," *Proceedings of the International Conference on Phenomena in Ionized Gases*, Vol. 4, Paris, 1963, pp. 511–512.

[2] Kerrebrock, J. L., "Nonequilibrium Ionization due to Electron Heating: I Theory," *AIAA Journal*, Vol. 2, No. 6, June 1964, pp. 1072–1080.

[3] Velichov, E. P., Dychne, A. U., and Shipuk, I. A., "Ionization Instability of a Plasma with Hot Electrons," *Proceedings of the 7th International Conference on Phenomena in Ionized Gases*, Vol. 2, Belgrade, 1965, pp. 675–681.

[4] Zampaglione, V., "Effect of an Electron Current along the Magnetic Field on the Development of Ionization Instability in a Low Temperature Plasma," *Plasma Physics*, Vol. 12, 1970, pp. 23–30.

[5] Solbes, A., Nakamura, T., and Kerrebrock, J. L., "Electrothermal Instability in Plasmas with Current Flow Parallel to the Magnetic Field," *Proceedings of the 11th Symposium on Engineering Aspects of Magnetohydrodynamics*, Pasadena, Calif., 1970, pp. 209215.

[6] Evans, R. H., Louis, J. F., Mitchner, M., and Kruger, C. H., "Ionization Instabilities in a Continuous Electrode Generator," *Proceedings of the 11th Symposium on Engineering Aspects of Magnetohydrodynamics*, Pasadena, Calif., 1970, pp. 191–192.

[7] Kerrebrock, J. L. and Draper, J., "Nonequilibrium MHD Generators with Molecular Gases," AIAA Paper 70-41, New York, 1970.

[8] Brederlow, G. and Witte, K. J., "Investigation of the Discharge Structure in a Rare Gas Alkali MHD Generator," *Proceedings of the 12th Symposium on Engineering Aspects of Magnetohydrodynamics*, Argonne, Ill., 1972, pp. I.9.1–I.9.6.

[9] Uncles, R. J. and Nelson, A. H., "Dynamic Stabilization of the Electrothermal Instability," *Plasma Physics*, Vol. 12, 1970, pp. 917–926.

[10] Sen, A. K., "Feedback Control of Ionization Instability in MHD Generators," *Energy Conversion*, Vol. 13, 1973, pp. 13–17.

[11] Belousov, V. N., Eliseev, V. V., and Shipuk, I. Ya., "Ionization Instability and Turbulent Conductivity on Nonequilibrium Plasma," *Proceedings of the 3rd International Conference on Magnetohydrodynamic Electrical Power Generation*, Vol. 2, Salzburg, 1966, pp. 323–334.

[12] Shipuk, I. Ya. and Pashkin, S. V., "Some Characteristics of an Unstable Quasi-Equilibrium Plasma in Crossed E and H Fields," *Proceedings of the 4th International Conference on Magnetohydrodynamic Electrical Power Generation*, Vol. 1, Warsaw, 1968, pp. 569–580.

[13] Vithshas, A. F., Golubev, V. S., and Malikov, M. M., "Investigation of Ionizational Instability in a Disk-shaped Hall Channel," *Proceedings of the 4th International Conference on Magnetohydrodynamic Electrical Power Generation*, Vol. 1, Warsaw, 1968, pp. 529–545.

[14] Malikov, M. M., "Experimental Investigation of Nonequilibrium Plasmas," *Teplofizika Vysokikh Temperatur*, Vol. 8, No. 2, 1970, pp. 260–265.

[15] Kasabov, G. A., "Closed Cycle MHD with Gaseous Working

Fluids Instabilities," *Proceedings of the 4th International Conference on Magnetohydrodynamic Electrical Power Generation,* Vol. 4, Warsaw, 1968, pp. 3555–3561.

[16] Zettwoog, P., "Flow and Nonequilibrium Ionization," *Proceedings of the 3rd International Conference on Magnetohydrodynamic Electrical Power Generation,* Vol. 2, Salzburg, 1966, pp. 303–317.

[17] Nelson, A. H. and Haines, M. G., "Analysis of the Nature and Growth of Electrothermal Waves," *Plasma Physics,* Vol. 11, 1969, pp. 811–837.

[18] Solbes, A., "Instabilities in Nonequilibrium MHD Plasmas, A Review," AIAA Paper 70-40, New York, 1970.

[19] Nakamura, T. and Riedmüller, W., "Investigation of a Non-equilibrium MHD Plasma under the Condition of Fully Ionized Seed," *Proceedings of the 5th International Conference on Magnetohydrodynamic Electrical Power Generation,* Vol. II, Munich, April 1971, pp. 291–302.

[20] Agnew, L. and Summers, C., "Quantitative Spectroscopy of Cesium Plasmas," *Proceedings of the 7th International Conference on Phenomena in Ionized Gases,* Vol. II, Belgrade, 1965, pp. 574–580.

[21] Frost, S. L., "Conductivity of Seeded Atmospheric Pressure Plasmas," *Journal of Applied Physics,* Vol. 32, 1961, pp. 2029–2039.

[22] Schweitzer, S. and Mitchner, M., "Electrical Conductivity of Partially Ionized Gases," *AIAA Journal,* Vol. 4, No. 6, June 1966, pp. 1012–1019.

[23] McCune, J., "Transport Properties of Partially Ionized Gases Using a Modified Frost's Mixture Rule," AMP 201, Aug. 1966, AVCO Everett Research Lab., Everett, Mass.

[24] Kruger, C. H., Mitchner, M., and Daybelge, U., "Transport Properties of MHD-Generator Plasmas," *AIAA Journal,* Vol. 6, No. 9, Sept. 1968, pp. 1712–1723.

[25] Frost, L. S. and Phelps, A. V., "Momentum-Transfer Cross Section for Slow Electrons in He, Ar, Kr, and Xe from Transport Coefficients," *The Physical Review,* Vol. 136A, 1964, pp. 1538–1545.

[26] Zampaglione, V., "Text of the Rapporteur," *Proceedings of the 5th International Conference on Magnetohydrodynamic Electrical Power Generation,* Munich, April 1971, pp. 244–250.

[27] Solbes, A., "Quasi-Linear Plane Wave Study of Electrothermal Instabilities," *Proceedings of a Symposium on Magnetohydrodynamic Electrical Power Generation,* Vol. 1, Warsaw, 1968, pp. 499–518.

[28] Brederlow, G., Zinko, H., and Witte, K. J., "Performance of the IPP Noble Gas Alkali MHD Generator and Investigation of the 'Streamers' in the Generator Duct," *Proceedings of the 5th International Conference on Magnetohydrodynamic Electrical Power Generation,* Vol. 2, Munich, 1971, pp. 387–401.